

Relaxation to the invariant density for the kicked rotor

Maxim Khodas and Shmuel Fishman

Department of Physics, Technion, Haifa 32000, Israel

Oded Agam

The Racah Institute for Physics, The Hebrew University, Jerusalem 91904, Israel

(Received 28 October 1999; revised manuscript received 17 May 2000)

The relaxation rates to the invariant density in the chaotic phase space component of the kicked rotor (standard map) are calculated analytically for a large stochasticity parameter K . These rates are the logarithms of the poles of the matrix elements of the resolvent, $\hat{R}(z) = (z - \hat{U})^{-1}$, of the classical evolution operator \hat{U} . The resolvent poles are located inside the unit circle. For hyperbolic systems this is a rigorous result, but little is known about mixed systems such as the kicked rotor. In this work, the leading relaxation rates of the kicked rotor are calculated in the presence of noise, to the leading order in $1/\sqrt{K}$. Then the limit of vanishing noise is taken and the relaxation rates are found to be finite, corresponding to poles lying inside the unit circle. It is found that the slow relaxation rates, in essence, correspond to diffusion modes in the momentum direction. Faster relaxation modes intermix the motion in the momentum and the angle space. The slowest relaxation rate of distributions in the angle space is calculated analytically by studying the dynamics of inhomogeneities projected down to this space. The analytical results are verified by numerical simulations.

PACS number(s): 05.45.Ac

I. INTRODUCTION

For chaotic systems specific trajectories are extremely complicated and look random [1]. Therefore it is natural to explore the statistical properties of such systems. For this purpose the evolution of probability densities of trajectories in phase space is studied [2–4]. For chaotic systems, the probability densities approach an equilibrium density that depends only on the system and not on the initial density. For hyperbolic systems (A systems), like the baker map, the relaxation is exponential. For such systems the existence of the relaxation rates was rigorously established and the relaxation rates are the Ruelle resonances [5–7]. To study these rates it is instructive to introduce the evolution operator of densities that is sometimes called the Frobenius-Perron (FP) operator. Relaxation to the equilibrium density is studied traditionally in statistical mechanics. In particular, for particles performing a random walk in a finite box, relaxation to the equilibrium uniform density takes place and is governed by the rate related to the lowest nontrivial mode of the diffusion equation. It is known that for the classical kicked rotor, described by the standard map, diffusive spread in phase space takes place for a sufficiently large stochasticity parameter [8,9]. Therefore it is natural to study the Frobenius-Perron operator for the kicked rotor and to compare it to the diffusion operator, a comparison that enables one to study some aspects of chaotic dynamics in the framework of statistical mechanics [10]. The kicked rotor model is a paradigm for the chaotic behavior of systems where one variable is unbounded in the phase space. For such classical systems, diffusive spreading takes place. For their quantum counterparts it is suppressed by interference effects, leading to a mechanism that is similar to Anderson localization in disordered solids [11–13].

The kicked rotor is defined by the Hamiltonian (in appropriate units)

$$\mathcal{H} = \frac{1}{2}J^2 + K \cos \theta \sum_n \delta(t-n), \quad (1)$$

where J is the angular momentum, θ is the conjugate angle ($0 \leq \theta < 2\pi$) and K is the stochasticity parameter. Since the angular momentum between the kicks is conserved, the equation of motion generated by the Hamiltonian (1) reduces to a map, known as the standard map

$$\bar{\theta} = \theta + \bar{J}, \quad (2)$$

$$\bar{J} = J - K \sin \theta, \quad (3)$$

where θ and J are the angle and the angular momentum before the kick, while $\bar{\theta}$ and \bar{J} are these quantities just before the next kick. For $K > K_c \approx 0.9716$, diffusion in phase space is found, and for large K the diffusion coefficient is given by an expansion in $1/\sqrt{K}$ as [14]

$$D(K) = \frac{K^2}{4} [1 - 2J_2(K) + \dots]. \quad (4)$$

To be precise, it was shown that after a large number of kicks n , the variance of the momentum behaves as

$$\langle (J - \langle J \rangle)^2 \rangle \sim 2Dn, \quad (5)$$

where $\langle \dots \rangle$ denotes an averaging over the angle initial distribution, and D is given by Eq. (4).

It is assumed that the system evolves in the presence of finite noise and the limit of the vanishing noise is taken in the end of the calculation. The noise is required here in order to get well defined results. It leads to escape from the accelerator modes and other stable islands. Accelerator modes, where the angular momentum J grows linearly with time, are found for values of K and the initial values (θ_0, J_0) of the

angle and the angular momentum, which satisfy $K \sin \theta_0 = 2\pi l_0$ and $J = 2\pi l$ where l and l_0 are integers. In such a situation, at each step J grows by $2\pi l_0$, as is obvious from Eqs. (2) and (3), namely, its growth is linear in time. For some values of K the point (θ_0, J_0) is stable and also for initial conditions in its vicinity the momentum grows linearly. This differs from diffusion, which takes place in the chaotic component of phase space. For trajectories in the chaotic component of phase space, noise avoids long time sticking in the vicinity of islands of stability [15]. In numerical calculations without noise, diffusion was found for $K > K_c$ for trajectories in the extended chaotic component for large values of K ; however, some exceptions were also reported [15]. The diffusion coefficient (4) was calculated in the presence of finite noise (in the long time limit) and the limit of the vanishing noise can be taken in the end of the calculation [14]. It describes the typical spreading of trajectories in the chaotic component. Since the kicked rotor is a mixed system, as is the case for most physical examples, the rigorous mathematical theory for relaxation [5,3,2] does not apply and one has to resort to heuristic methods.

In the present paper [16], the Frobenius-Perron operator will be calculated for the kicked rotor on the torus:

$$\begin{aligned} (0 \leq J < 2\pi s), \\ (0 \leq \theta < 2\pi), \end{aligned} \quad (6)$$

where s is an integer. This is reasonable since the map [Eqs. (2) and (3)] is 2π periodic in both in J and in θ . The operator is defined in the space spanned by the Fourier basis as

$$\phi_{km} = (J\theta|km) = \frac{1}{\sqrt{2\pi}} \frac{1}{\sqrt{2\pi s}} \exp(im\theta) \exp\left(i \frac{kJ}{s}\right). \quad (7)$$

Note that the functions ϕ_{k0} form the basis of eigenstates of the diffusion operator in the angular momentum J . The FP operator for an area preserving and invertible map,

$$\bar{\mathbf{x}} = M(\mathbf{x}),$$

is

$$\hat{U}\rho(\theta, J) = \rho(M^{-1}(\theta, J)). \quad (8)$$

It was studied rigorously for the hyperbolic systems and many of its properties are known [2,3,5,17,18]. It is a unitary operator in \mathcal{L}^2 , the Hilbert space of square integrable functions. Therefore its resolvent

$$\hat{R}(z) = \frac{1}{z - \hat{U}} = \frac{1}{z} \sum_{n=0}^{\infty} \hat{U}^n z^{-n} \quad (9)$$

is singular on the unit circle in the complex z plane. The matrix elements of \hat{R} are discontinuous there and one finds a jump between two Riemann sheets. This results from the fact that the spectrum is continuous and infinitely degenerate [2]. The sum (9) is convergent for $|z| > 1$, therefore it identifies the physical sheet as the one connected with the region $|z| > 1$. (This is analogous to the sign of the small imaginary increment in the energy that is used in the definition of the

Green function). The Ruelle resonances are the poles of the matrix elements of the resolvent, on the Riemann sheet, extrapolated from $|z| > 1$ [17]. These describe the decay of smooth probability distribution functions to the invariant density in a coarse grained form [3,5]. Even a smooth initial distribution will develop complicated patterns as a result of the evolution of a chaotic map. The Ruelle resonances describe the decay of its coarse grained form to the invariant density. In spite of the solid mathematical theory there are very few examples where the Ruelle resonances were calculated for specific systems. They were calculated analytically for the baker map where the basis of Legendre polynomials was used [17] and its various variants [3]. The Ruelle resonances were also calculated for the ‘‘cat’’ map and some of its variants [18]. Blum and Agam applied a variational method for the calculation of the leading Ruelle resonances of the ‘‘perturbed cat’’ map, and the results were verified numerically [19]. In addition, they calculated the leading resonances of the standard map with $s = 1$ for various values of the stochasticity parameter K . The leading Ruelle resonances for the kicked top were calculated by Weber, Haake, and Šeba [20] with the help of a combination of a cycle expansion and numerical calculations. The resonances mentioned above are not related to the spectrum of the Liouville operator that is confined to the unit circle because of its unitarity.

In the present work, the FP operator is calculated for the kicked rotor. Here the classical evolution operator, for one time step, can be written in the form

$$\hat{U}_{KR} = \delta(\bar{\theta} - \theta - \bar{J}) \delta(\bar{J} - J + K \sin \theta), \quad (10)$$

and its operation on a phase space density ρ is

$$\hat{U}\rho(\theta, J) = \rho(\theta - J, J + K \sin(\theta - J)). \quad (11)$$

To make the calculation well defined, noise is added to the system. It is shown that the noise acts effectively as coarse graining and the resulting FP operator is not unitary (see also [21]). For large stochasticity parameter K , we show that the slowest relaxation modes in the limit of infinitesimal noise are the modes of the diffusion operator in the angular momentum space. Also calculated is the slowest rate of relaxation in the angle space. The approximate analytical results are tested numerically.

It is understood that the noise is kept finite when the limits of large K and s are taken and then the limit of zero noise is taken. The natural question is whether it is possible that this description, which was established only for hyperbolic systems, also holds for mixed systems. Clearly, for mixed systems it can only be approximate. It holds for large values of the stochasticity parameter K since then most of the phase space is covered by the chaotic component. For smaller values of K the weight of the regular regions increases. In such a situation, in the limit of increasing resolution the resonances related to the regular component are expected to move to the unit circle in the complex z plane, corresponding to the quasiperiodic motion, while the resonances associated with the chaotic component stay inside the unit circle. This was found by Weber, Haake, and Šeba [20] for the kicked top that is a mixed system.

How is the FP operator related to the quantum mechanical evolution operator? It was shown numerically for the baker map that if both operators are calculated with finite resolution they exhibit the same Ruelle resonances [21]. In this calculation it was assumed that the phase space coarse graining tends to zero in the semiclassical limit $\hbar \rightarrow 0$. It was shown by Zirnbauer [22] that some noise is required for a meaningful definition of the field theories introduced to study level statistics for chaotic systems [23]. This noise affects only quantum properties; therefore, the resulting ensemble has the same classical FP operator. The localization length of the kicked rotor calculated from this field theory [24] is related to the classical FP operator. This operator is analyzed in the present work, clarifying some issues of that work. The results hold only for typical quantum systems, since the noise introduced in the present work as well as the noise required for the stabilization of the field theory [22] washes out the sensitive quantum details, such as the number theoretical properties of the effective Planck constant [25].

The Frobenius-Perron operator in the basis (7) in the presence of noise is defined and calculated in Sec. II, its Ruelle resonances are obtained within some approximations in Sec. III and their regime of validity is tested numerically in Sec. IV. The results are summarized and discussed in Sec. V.

II. THE EVOLUTION OPERATOR OF PHASE SPACE DISTRIBUTIONS

In this section, the evolution operator of phase space densities of the kicked rotor in the presence of some type of noise is derived. The noise is added to the free motion part (2). In the absence of noise the phase space evolution of a distribution f is given by Liouville equation

$$\frac{df}{dt} = \frac{\partial f}{\partial t} + \dot{\theta} \frac{\partial f}{\partial \theta} + J \frac{\partial f}{\partial J} = 0. \quad (12)$$

If noise that conserves J , and leads to diffusion in θ , is added to the free motion, Eq. (12) should be replaced by

$$\frac{\partial f}{\partial t} + J \frac{\partial f}{\partial \theta} - \frac{\sigma^2}{2} \frac{\partial^2 f}{\partial \theta^2} = 0, \quad (13)$$

where $J = \dot{\theta}$ was used. It can be written as

$$\frac{\partial f}{\partial t} = \hat{A}f, \quad (14)$$

where the operator \hat{A} is

$$\hat{A} = -J \frac{\partial}{\partial \theta} + \frac{\sigma^2}{2} \frac{\partial^2}{\partial \theta^2}. \quad (15)$$

The complete set of its eigenfunctions is given by $\varphi_m = (1/\sqrt{2\pi})\exp(im\theta)$, where m is an integer. The operator we need is $\hat{U}_{noise} = e^{\hat{A}}$, and explicitly

$$(J' \theta' | \hat{U}_{noise} | J \theta) = \sum_m \varphi_m(\theta') \varphi_m^*(\theta) \exp(\alpha_m) \delta(J - J'), \quad (16)$$

where the α_m are the eigenvalues of the operator \hat{A} , namely $\hat{A}|\varphi_m\rangle = \alpha_m|\varphi_m\rangle$. Obviously

$$\alpha_m = -imJ - \frac{\sigma^2}{2} m^2 \quad (17)$$

leading to

$$(J' \theta' | \hat{U}_{noise} | J \theta) = \sum_m \frac{1}{2\pi} \exp\left(im(\theta' - \theta - J) - \frac{\sigma^2}{2} m^2\right) \times \delta(J - J'). \quad (18)$$

The δ function in momentum reflects the fact that the noise does not affect the momentum. The matrix elements $(k_2 m_2 | \hat{U} | k_1 m_1)$ of the evolution operator \hat{U} in the Fourier basis (7) will be calculated in two steps, first the contribution of the kick, and then the one of the free motion with noise will be calculated. According to Eqs. (3) and (11), the kick transforms the state

$$(J \theta | k_1 m_1) = \frac{1}{\sqrt{2\pi}} \frac{1}{\sqrt{2\pi s}} \exp(im_1 \theta) \exp\left(i \frac{k_1 J}{s}\right)$$

to the state

$$\frac{1}{\sqrt{2\pi}} \frac{1}{\sqrt{2\pi s}} \exp(im_1 \theta) \exp\left(i \frac{k_1}{s} (J + K \sin \theta)\right) \equiv (J \theta | \hat{U}_K | k_1 m_1). \quad (19)$$

Adding the effect of noise yields the matrix element in the mixed representation

$$(J \theta | \hat{U} | k_1 m_1) = \int_0^{2\pi} d\theta' \int_0^{2\pi s} dJ' (J \theta | \hat{U}_{noise} | J' \theta') \times (J' \theta' | \hat{U}_K | k_1 m_1). \quad (20)$$

Its transformation to the basis (7) is calculated in Appendix A and the result is

$$(k_2 m_2 | \hat{U} | k_1 m_1) = J_{m_2 - m_1} \left(\frac{k_1 K}{s}\right) \exp\left(-\frac{\sigma^2}{2} m_2^2\right) \delta_{k_2 - k_1, m_2 s}. \quad (21)$$

For $\sigma = 0$, using Eq. (21) one can verify by a straightforward summation that $\hat{U}^\dagger \hat{U} = I$; therefore, the operator is unitary as required.

Some of the eigenfunctions of \hat{U} in the limit $\sigma = 0$ are easily found. It is convenient to use the representation (10) of \hat{U} . We guess an eigenfunction of the form

$$F(\theta, J) = \delta(\theta - \theta_0) \sum_l \exp(iqJ/s) \delta(J - 2\pi l), \quad (22)$$

with the q integer satisfying $1 \leq q \leq s$. These are functions that are localized on accelerator modes representing linear growth of the angular momentum with time. To check that these are indeed eigenfunctions, we note that

$$\begin{aligned} \hat{U}_{KR}F(\theta, J) &= \delta(\theta - J - \theta_0) \sum_T \delta(J + K \sin \theta_0 - 2\pi l) \\ &\times \exp\left(i \frac{q}{s} (J + K \sin \theta_0)\right), \end{aligned} \quad (23)$$

taking θ_0 so that

$$K \sin \theta_0 = 2\pi l_0,$$

where l_0 is an integer yielding

$$\hat{U}_{KR}F(\theta, J) = e^{i2\pi q l_0/s} F(\theta, J), \quad (24)$$

since the right-hand side (RHS) of Eq. (23) does not vanish only for $J = 2\pi l$. The eigenvalues $e^{i2\pi q l_0/s}$ lie on the unit circle and become dense as $s \rightarrow \infty$. There are more eigenfunctions of this form located on other periodic orbits [26].

III. IDENTIFICATION OF THE RUELLE RESONANCES

The purpose of this section is to calculate the Ruelle resonances for the kicked rotor with the help of the Frobenius-Perron operator (21). The calculation will be done for finite noise σ and then the limit $\sigma \rightarrow 0$ will be taken. The Ruelle resonances are the poles of matrix elements of the resolvent operator \hat{R} of Eq. (9),

$$R_{12} = (k_1 m_1 | \hat{R}(z) | k_2 m_2) = \left(k_1 m_1 \left| \frac{1}{z - \hat{U}} \right| k_2 m_2 \right), \quad (25)$$

when analytically continued from outside of the unit circle in the complex plane. It is useful to introduce the operator

$$\hat{R}'(z) = \frac{1}{1 - z\hat{U}}, \quad (26)$$

which is related to the resolvent by

$$\frac{1}{z} \hat{R}'\left(\frac{1}{z}\right) = \hat{R}(z) \quad (27)$$

and

$$\frac{1}{z} \hat{R}\left(\frac{1}{z}\right) = \hat{R}'(z). \quad (28)$$

The matrix elements of \hat{R} and \hat{R}' satisfy similar relations. Continuing the matrix elements of $\hat{R}(z)$ from the outside to the inside of the unit circle is equivalent to continuing the matrix elements of $\hat{R}'(z)$ from the inside to the outside of the unit circle. The last continuation is easier to study since the expansion

$$\hat{R}'(z) = \frac{1}{1 - z\hat{U}} = \sum_{n=0}^{\infty} z^n \hat{U}^n \quad (29)$$

is convergent inside the unit circle, because

$$\|z\hat{U}\| \leq 1. \quad (30)$$

The resulting matrix elements are

$$R'_{12} = (k_1 m_1 | \hat{R}'(z) | k_2 m_2) = \sum_{n=0}^{\infty} a_n z^n, \quad (31)$$

where

$$a_n = (k_1 m_1 | \hat{U}^n | k_2 m_2). \quad (32)$$

Through Eqs. (27) and (28) this expansion is related to matrix elements outside of the unit circle. If z_c is a singularity of R_{12} , then $1/z_c$ is a singular point of R'_{12} . Consequently the first singularity of the analytic continuation of $R'_{12}(z)$ from the inside to the outside of the unit circle gives the first singularity one encounters when analytically continuing $R_{12}(z)$ from outside to inside the unit circle, i.e. it is just the leading nontrivial resonance. This is the most interesting resonance determining the relaxation to the invariant density. The first singularity in the extrapolation of the matrix elements of \hat{R}' from the inside to the outside of the unit circle is determined from the fact that it is the radius of convergence of this series. Moreover, according to the Cauchy-Hadamard theorem (see [27]) the inverse of the radius of convergence is given by

$$r^{-1} = \limsup_{n \rightarrow \infty} \sqrt[n]{|a_n|}. \quad (33)$$

If $a_n \sim c/r^n$ we may say that the radius of convergence is the asymptotic value of a_{n-1}/a_n . This is the basis for the ratio method for determining the radius of convergence. The resonance that is closest to the unit circle can be identified from the radius of convergence.

We turn now to calculate the coefficients a_n . First the matrix elements $(k_0 | \hat{R}'(z) | k_0)$ will be calculated. For these, the expansion coefficients are

$$a_n = (k_0 | \hat{U}^n | k_0). \quad (34)$$

Introducing the resolution of the identity,

$$\begin{aligned} a_n &= \sum_{k_1, m_1} \sum_{k_2, m_2} \cdots \sum_{k_{n-1}, m_{n-1}} (k_0 | \hat{U} | k_1 m_1) \\ &\times (k_1 m_1 | \hat{U} | k_2 m_2) \cdots (k_{n-1} m_{n-1} | \hat{U} | k_0), \end{aligned} \quad (35)$$

and substitution of the evolution operator (21) leads to

$$\begin{aligned} a_n &= \sum_{k_1, m_1} \sum_{k_2, m_2} \cdots \sum_{k_{n-1}, m_{n-1}} \\ &\times J_{0-m_1} \left(\frac{k_1 K}{s} \right) \delta_{k-k_1, 0} J_{m_1-m_2} \left(\frac{k_2 K}{s} \right) \\ &\times \exp\left(-\frac{\sigma^2}{2} m_1^2\right) \delta_{k_1-k_2, m_1 s} \\ &\times J_{m_2-m_3} \left(\frac{k_3 K}{s} \right) \exp\left(-\frac{\sigma^2}{2} m_2^2\right) \\ &\times \delta_{k_2-k_3, m_2 s} \cdots J_{m_{n-1}-0} \left(\frac{k K}{s} \right) \\ &\times \exp\left(-\frac{\sigma^2}{2} m_{n-1}^2\right) \delta_{k_{n-1}-k, m_{n-1} s}. \end{aligned} \quad (36)$$

Summation over the k_i yields

$$\begin{aligned}
a_n = & \sum_{m_1} \sum_{m_2} \dots \sum_{m_{n-1}} J_{0-m_1} \left(\frac{kK}{s} \right) \\
& \times J_{m_1-m_2} \left(\frac{kK}{s} - m_1 K \right) \exp \left(-\frac{\sigma^2}{2} m_1^2 \right) \\
& \times J_{m_2-m_3} \left(\frac{kK}{s} - (m_1+m_2) K \right) \\
& \times \exp \left(-\frac{\sigma^2}{2} m_2^2 \right) \dots \\
& \times J_{m_{n-2}-m_{n-1}} \left(\frac{kK}{s} - (m_1+m_2+\dots+m_{n-2}) K \right) \\
& \times \exp \left(-\frac{\sigma^2}{2} m_{n-2}^2 \right) J_{m_{n-1}-0} \left(\frac{kK}{s} \right) \\
& \times \exp \left(-\frac{\sigma^2}{2} m_{n-1}^2 \right) \delta_{m_1+m_2+\dots+m_{n-2}+m_{n-1},0}.
\end{aligned} \tag{37}$$

Thus in order to obtain the expansion coefficient a_n we should perform summation in Eq. (37) over all integers subject to the constraint

$$m_1 + m_2 + \dots + m_{n-1} = 0. \tag{38}$$

We are interested in the limit of large s and K . The limits are taken in the order

$$(1) s \rightarrow \infty, \quad (2) K \rightarrow \infty, \quad (3) \sigma \rightarrow 0. \tag{39}$$

Finite σ is required to assure the absolute convergence of the series. Therefore Eq. (37) is summed for finite σ and the limit $\sigma \rightarrow 0$ should be taken in the end of the calculation. Having this limit in mind, the leading term in K/s and $1/\sqrt{K}$ will be identified. It will be assumed that the mode that is calculated is sufficiently low so that

$$0 < kK/s \ll 1. \tag{40}$$

Each term in Eq. (37) is defined by the string

$$(m_1, m_2, \dots, m_i, \dots, m_{n-1}).$$

The leading contribution

$$a_n^{(0)} = J_0^n \left(\frac{kK}{s} \right) \approx \left(1 - \frac{k^2 K^2}{4s^2} \right)^n \tag{41}$$

results from the string where all m_j vanish. A nonvanishing m_j results in a Bessel function with a large argument, since $K/s \ll 1$ and $K \gg 1$, and therefore it leads to a factor $1/\sqrt{K}$ in the contribution to a_n . Let m_i be the first nonvanishing m_j and m_f the last nonvanishing one. The first factor in Eq. (37) that is not $J_0(kK/s)$ is $J_{-m_i}(kK/s)$, and the last factor that differs from $J_0(kK/s)$ is

$$J_{m_f} \left(\frac{kK}{s} - (m_1 + m_2 + \dots + m_f) K \right) = J_{m_f} \left(\frac{kK}{s} \right). \tag{42}$$

Since $J_n(x) \approx (x^n/2^n n!)$ for small x and $J_{-n}(x) = (-1)^n J_n(x)$, the contribution of the terms between i and f is of the order

$$C \left(\frac{kK}{s} \right)^{|m_i|+|m_f|}, \tag{43}$$

where C is the contribution of the factors with m_j that are not the first and last ones. The first factor after m_i is

$$J_{m_i-m_{i+1}} \left(\frac{kK}{s} - (m_1 + \dots + m_i) K \right) = J_{m_i-m_{i+1}} \left(\frac{kK}{s} - m_i K \right)$$

and the last factor before m_f is

$$\begin{aligned}
& J_{m_{f-1}-m_f} \left(\frac{kK}{s} - (m_1 + \dots + m_{f-1}) K \right) \\
& = J_{m_{f-1}-m_f} \left(\frac{kK}{s} - (m_i + \dots + m_{f-1}) K \right).
\end{aligned}$$

The terms in between are of the form $J_{m_{j-1}-m_j}((kK/s) - M_j K)$, where $M_j = m_i + m_{i+1} + \dots + m_j \neq 0$ that are of the order $1/\sqrt{K}$. Therefore the largest contribution from a string m_i, m_{i+1}, \dots, m_f is from the shortest string, namely, $f = i + 1$. Because of Eq. (38) $m_i = -m_f$ and because of Eq. (43) the leading contribution is from the string $m_i = -m_f = \pm 1$. The resulting contribution is

$$C = J_{m_i-m_f} \left(\frac{kK}{s} - m_i K \right) = J_{\pm 2} \left(\frac{kK}{s} - (\pm 1) K \right) \approx J_2(K). \tag{44}$$

The string can start at $n-2$ places, therefore the leading correction to $a_n^{(0)}$ is

$$a_n^{(1)} = 2(n-2) J_0^{n-3} \left(\frac{kK}{s} \right) J_2 \left(\frac{kK}{s} - K \right) J_1^2 \left(\frac{kK}{s} \right) e^{-\sigma^2},$$

which is approximated as

$$a_n^{(1)} \approx 2(n-2) \left(1 - \frac{k^2 K^2}{4s^2} \right)^{n-3} J_2(K) \left(\frac{kK}{2s} \right)^2 e^{-\sigma^2}. \tag{45}$$

The sum of the contributions (41) and (45) is

$$\begin{aligned}
a_n^{(0)} + a_n^{(1)} &\sim \left(1 - \frac{k^2 K^2}{4s^2}\right)^n + 2n \left(1 - \frac{k^2 K^2}{4s^2}\right)^{n-1} J_2(K) \\
&\quad \times \exp\left(-\frac{\sigma^2}{2} m_{n-2}^2\right) J_{m_{n-1}-m'}\left(\frac{k'K}{s}\right) \exp\left(-\frac{\sigma^2}{2} m_{n-1}^2\right) \\
&\quad \times \delta_{(m+m_1+m_2+\dots+m_{n-2}+m_{n-1})s, k-k'}. \quad (52)
\end{aligned}$$

$$\begin{aligned}
&\times \left(\frac{kK}{2s}\right)^2 e^{-\sigma^2 \left(\frac{n-2}{n}\right) \left[\frac{1}{1 - \frac{k^2 K^2}{4s^2}}\right]^2}. \quad (46)
\end{aligned}$$

In the leading order $[1 - (k^2 K^2/4s^2)]^{-1} \approx 1$ and

$$\lim_{n \rightarrow \infty} \frac{n-2}{n} = 1.$$

Therefore in the leading order

$$\begin{aligned}
a_n^{(0)} + a_n^{(1)} &\sim \left[\left(1 - \frac{k^2 K^2}{4s^2}\right) + 2J_2(K) \left(\frac{kK}{2s}\right)^2 e^{-\sigma^2} \right]^n \\
&= \left[1 - \frac{k^2 K^2}{4s^2} (1 - 2J_2(K) e^{-\sigma^2}) \right]^n. \quad (47)
\end{aligned}$$

The resonance closest to the unit circle, z_k , is identified from Eq. (33) as the inverse of the radius of convergence

$$z_k = 1 - \frac{k^2 K^2}{4s^2} + \frac{k^2 K^2}{4s^2} 2J_2(K) e^{-\sigma^2}, \quad (48)$$

or within this order of the calculation as

$$z_k = \exp\left(-\frac{k^2 K^2}{4s^2} (1 - 2J_2(K) e^{-\sigma^2})\right). \quad (49)$$

These are the eigenvalues of the diffusion operator with the diffusion coefficient

$$D(K) = \frac{K^2}{4} (1 - 2J_2(K) e^{-\sigma^2}), \quad (50)$$

in agreement with the earlier results [14].

The analysis of the off-diagonal matrix elements

$$a_n = (km | \hat{U}^n | k'm') \quad (51)$$

is similar. We assume again inequality (40) and $K \gg 1$. Analogously to Eq. (37), one obtains

$$\begin{aligned}
a_n &= \sum_{m_1} \sum_{m_2} \dots \sum_{m_{n-1}} J_{m-m_1} \left(\frac{kK}{s} - mK\right) \exp\left(-\frac{\sigma^2}{2} m^2\right) \\
&\quad \times J_{m_1-m_2} \left(\frac{kK}{s} - (m+m_1)K\right) \\
&\quad \times \exp\left(-\frac{\sigma^2}{2} m_1^2\right) J_{m_2-m_3} \left(\frac{kK}{s} - (m+m_1+m_2)K\right) \\
&\quad \times \exp\left(-\frac{\sigma^2}{2} m_2^2\right) \dots \\
&\quad \times J_{m_{n-2}-m_{n-1}} \left(\frac{kK}{s} - (m+m_1+m_2+\dots+m_{n-2})K\right)
\end{aligned}$$

Because of the last δ function, $a_n \neq 0$ only if $(k-k')/s = q$ is an integer. The leading contribution results from the string $m_1 = -m$, $m_{n-1} = q$ and all other m_j vanish. It is therefore of the form

$$a_n^{(0)} = B J_0^{n-4} \left(\frac{kK}{s}\right), \quad (53)$$

where

$$\begin{aligned}
B &= J_{2m}(mK) J_{-m} \left(\frac{kK}{s}\right) J_{-q} \left(\frac{kK}{s}\right) J_{q-m'} \left(\frac{k'K}{s}\right) \\
&\quad \times \exp(-\sigma^2 m^2) \exp\left(-\frac{\sigma^2}{2} q^2\right), \quad (54)
\end{aligned}$$

which behaves as $a_n^{(0)}$ of Eq. (41) in the large n limit. The leading correction is found from neighboring pairs $m_i = -m_{i+1} = \pm 1$ as in the case studied before with a result similar to the approximation (45) for $a_n^{(1)}$ in the large n limit. Therefore no new resonances are found from the off-diagonal terms with $k \neq 0$, in the order of approximation that was used.

For $s \gg 1$ the diffusion modes in momentum space constitute the slow degrees of freedom of the system. However, the faster relaxation modes (or, alternatively, the modes of a system with $s \approx 1$) cease to be angle independent. To evaluate the magnitude of such a fast relaxation rate within our perturbation scheme, we have to calculate matrix elements associated with the relaxation of disturbances from the invariant density that involve functions from the angular subspace $\{|0, m\rangle\}$ with $m \neq 0$. Consider, therefore, the matrix element

$$a_n = (0m | \hat{U}^n | km'). \quad (55)$$

The equation corresponding to Eq. (36) is:

$$\begin{aligned}
a_n &= \sum_{k_1, m_1} \sum_{k_2, m_2} \dots \sum_{k_{n-1}, m_{n-1}} (0m | \hat{U} | k_1 m_1) \\
&\quad \times (k_1 m_1 | \hat{U} | k_2 m_2) \dots (k_{n-1} m_{n-1} | \hat{U} | km') \\
&= \sum_{k_1, m_1} \sum_{k_2, m_2} \dots \sum_{k_{n-1}, m_{n-1}} J_{m-m_1} \left(\frac{k_1 K}{s}\right) \\
&\quad \times \exp\left(-\frac{\sigma^2}{2} m^2\right) \delta_{-k_1, ms} J_{m_1-m_2} \left(\frac{k_2 K}{s}\right) \\
&\quad \times \exp\left(-\frac{\sigma^2}{2} m_1^2\right) \delta_{k_1-k_2, m_1 s} J_{m_2-m_3} \left(\frac{k_3 K}{s}\right) \\
&\quad \times \exp\left(-\frac{\sigma^2}{2} m_2^2\right) \delta_{k_2-k_3, m_2 s} \dots J_{m_{n-1}-m'} \left(\frac{kK}{s}\right) \\
&\quad \times \exp\left(-\frac{\sigma^2}{2} m_{n-1}^2\right) \delta_{k_{n-1}-k, m_{n-1} s} \quad (56)
\end{aligned}$$

and summation over the k_i yields a nonvanishing result only if $k/s \equiv q$ is an integer. In this case,

$$\begin{aligned}
a_n &= \sum_{m_1} \sum_{m_2} \dots \sum_{m_{n-1}} J_{m-m_1}(-mK) \\
&\times \exp\left(-\frac{\sigma^2}{2}m^2\right) J_{m_1-m_2}((-m-m_1)K) \\
&\times \exp\left(-\frac{\sigma^2}{2}m_1^2\right) J_{m_2-m_3}((-m-m_1-m_2)K) \\
&\times \exp\left(-\frac{\sigma^2}{2}m_2^2\right) \dots \\
&\times J_{m_{n-2}-m_{n-1}}((-m-m_1-m_2-\dots-m_{n-2})K) \\
&\times \exp\left(-\frac{\sigma^2}{2}m_{n-2}^2\right) \\
&\times J_{m_{n-1}-m'}(qK) \exp\left(-\frac{\sigma^2}{2}m_{n-1}^2\right) \\
&\times \delta_{-m-m_1-m_2-\dots-m_{n-2}-m_{n-1},q}. \tag{57}
\end{aligned}$$

The result is independent of s . This is a sum over m_i constrained by

$$m + m_1 + m_2 + \dots + m_{n-2} + m_{n-1} = -q. \tag{58}$$

In every particular term in this multiple series, generally, we will have multiples of terms $J_\nu(MK)$. If $M=0$ and $\nu \neq 0$, such a term vanishes, while if both M and ν do not vanish $J_\nu(MK) \sim (1/\sqrt{K})$. The leading contribution is from sequences with the maximal number of factors $J_0(0)=1$. To identify these, we denote $J_0(0)=1$ by ‘‘1’’ and other factors by ‘‘x.’’ In this way, to every term in Eq. (57) corresponds the sequence of n symbols

$$x^*x^*1^*x^*x^*x^*1^*x^*1^*x^*x^*\dots1^*x^*x. \tag{59}$$

A crucial restriction is that if $m \neq 0$, two ‘‘1’’ symbols cannot be nearest neighbors as is shown in what follows. If $m \neq 0$ the sequence starts with ‘‘x’’ as is clear from Eq. (57). Let the i th symbol be ‘‘1.’’ Then

$$J_{m_{i-1}-m_i}((-m_1-m_2-\dots-m_{i-1})K) = J_0(0). \tag{60}$$

The previous term is

$$J_{m_{i-2}-m_{i-1}}((-m_1-m_2-\dots-m_{i-2})K). \tag{61}$$

For both to be $J_0(0)$ it is required that $m_{i-1}=0$, and $m_{i-2}-m_{i-1}=0$, implying $m_{i-2}=0$ resulting in

$$J_{m_{i-3}}((-m_1-m_2-\dots-m_{i-3})K) = 0,$$

for $m_{i-3} \neq 0$. Therefore if the term before the i th one is ‘‘1’’ (and we have two neighbors that are ‘‘1’’s) either m_{i-3} , and all m_j with $j < i-2$, vanish and all factors before the i th are ‘‘1’’s, in contradiction with the fact that for $m \neq 0$ the sequence starts with an x , or the contribution of the sequence vanishes (when one of the m_j does not vanish). Now one has

to find the strings (59) with the maximal number of ‘‘1’’s subject to given values of m , m' , and q . For this purpose strings with alternating ‘‘x’’ and ‘‘1’’ are constructed.

The ‘‘x’’ represent factors $J_{m_l-m_{l+1}}(-M_lK)$ where $M_l = m + \sum_{i=1}^l m_i$ and we have to choose the m_i so that the $J_{m_l-m_{l+1}}(-M_lK)$ are of maximal magnitude. Consider the string

$$\begin{aligned}
&\dots J_{m_l-m_{l+1}}(-M_lK) J_{m_{l+1}-m_{l+2}}(-M_{l+1}K) \\
&\times J_{m_{l+2}-m_{l+3}}(-M_{l+2}K) J_{m_{l+3}-m_{l+4}}(-M_{l+3}K) \dots \tag{62}
\end{aligned}$$

where the factors $\exp(-(\sigma^2/2)m_l^2)$ were omitted for the sake of brevity. Requiring that the second and fourth factors are ‘‘1’’ yields $m_{l+1}=m_{l+2}$ and $m_{l+3}=m_{l+4}$ as well as $M_{l+1}=M_{l+3}=0$. Therefore $M_l=-m_{l+1}$ and $M_{l+2}=m_{l+2}=-m_{l+3}$. This implies $m_{l+1}=m_{l+2}=-m_{l+3}=-m_{l+4} \equiv m^*$, and this string takes the form

$$\dots J_{m_l-m^*}(m^*K) J_0(0) J_{2m^*}(-m^*K) J_0(0) \dots \tag{63}$$

Continuation of the string to the left requires $m_l = -m^*$. The factors ‘‘x’’ are $J_{2m^*}(-m^*K) = J_{-2m^*}(m^*K) = J_{2m^*}(m^*K)$. For each value of K we choose the value of m^* so that $|J_{2m^*}(m^*K)|$ is maximal, namely,

$$|J_{2m^*}(m^*K)| = \max_m |J_{2m}(mK)|. \tag{64}$$

Now one is left to match this string to the ends that are determined by m , m' , and q . The term (57) is the sum of terms of the form

$$C^{(l)}(m, m^*) [J_{2m^*}(m^*K) \exp(-\sigma^2 m^{*2})]^{n'} C^{(r)}(m^*, m', q), \tag{65}$$

where n' is an integer of the order $n/2$. The string (63) is of period 4, and therefore the end terms are also of period 4 in n . One can always find enough values of m_i in the beginning and in the end of strings in Eq. (57) so that they take the form (65). The end terms $C^{(l)}(m, m^*)$ and $C^{(r)}(m^*, m', q)$ are sums of the contributions of these m_i . Some of the contributions to the end terms are presented in Appendix B. The end terms do not affect the resonance. Therefore the largest resonance associated with the fast decaying modes, corresponding to the slowest one, is up to the fourth root of the identity

$$\tilde{z} = \sqrt[4]{J_{2m^*}(m^*K) \exp\left(-\frac{\sigma^2}{2}m^{*2}\right)}, \tag{66}$$

independent of m , m' , and q . The reason that \tilde{z} is determined only up to the fourth root of the identity is the period 4 of the string (63). The resonances associated with the other fast decaying modes cannot be determined in the framework of the perturbative expansion of the present work.

The Frobenius-Perron operator is the evolution operator \hat{U} in the limit of vanishing noise. Therefore the Ruelle resonances are the poles of matrix elements of the resolvent \hat{R} in this limit. They form several groups. There is

$$z_0 = 1, \tag{67}$$

which is related to the equilibrium state found for $m=m'=q=0$. The resonances corresponding to the relaxation modes related to the diffusion in the angular momentum space are given by

$$z_k = \exp\left(-\frac{k^2 K^2}{4s^2} [1 - 2J_2(K)]\right). \quad (68)$$

Finally, the largest resonance related to relaxation in the θ direction is, up to the fourth root of the identity,

$$\tilde{z} = \sqrt[4]{J_{2m^*}(m^*K)}, \quad (69)$$

where m^* is chosen so that the expression is maximal for a given value of K . The corresponding relaxation rates γ_k and $\tilde{\gamma}$ are defined by

$$z_k = e^{-\gamma_k} \quad (70)$$

and by

$$|\tilde{z}| = e^{-\tilde{\gamma}}, \quad (71)$$

leading to $\gamma_k = |\ln z_k|$ and $\tilde{\gamma} = |\ln |\tilde{z}||$. The last resonance may take the four values

$$\tilde{z} = \pm e^{-\tilde{\gamma}}, \quad (72)$$

and

$$\tilde{z} = \pm i e^{-\tilde{\gamma}}. \quad (73)$$

The perturbative calculation enables one to compute only $|\tilde{z}|$.

IV. NUMERICAL EXPLORATION OF RELAXATION

In Sec. III the Ruelle resonances were calculated for large K and extrapolated from finite to vanishing variance of the noise σ . Finite noise has the effect of truncation of the matrix of the FP operator and the limit $\sigma \rightarrow 0$ is the infinite matrix limit. In the limit $K \rightarrow \infty$ complete stochasticity takes place, while for finite K the system is a mixed one, but for large K the chaotic component covers nearly all of phase space. The results of Sec. III were obtained as the leading terms in an expansion in powers of $1/\sqrt{K}$. In the present section, the results will be tested numerically for finite K and $\sigma=0$. The phase space (6) with various values of s will be used. The resonances of the type (70), corresponding to diffusion in angular momentum J and of the type (71) corresponding to relaxation in the θ direction will be calculated numerically from the relaxation rates of various perturbations to the uniform invariant density. For large s , the relaxation of the diffusion modes (70) (with small k) is slow and these dominate the long time behavior. To see the angular relaxation modes (71) one has to eliminate the slow relaxation. This can be done either by the choice of small s or by the use of distributions that are uniform in the momentum J . Evolving an initial distribution g for n time steps and projecting it on a distribution f defines the correlation function

$$C_{fg}(n) = (f | \hat{U}^n | g). \quad (74)$$

For a chaotic system, for large n it is expected to decay as

$$C_{fg}(n) \sim e^{-\gamma n}, \quad (75)$$

and the relaxation rate γ is computed numerically from plots of $C_{fg}(n)$ as a function of n . In what follows the distributions g and f will be selected from the Fourier basis (7) so that γ is expected to take the values γ_k or $\tilde{\gamma}$. Relaxation of the form (75) is expected to hold in the chaotic component. An efficient way to calculate correlation functions like (74) projected on this component is from a trajectory in phase space. By ergodicity it samples all phase space in this component. The phase space integrals involved in the calculation of Eq. (74) are replaced by time averages along the trajectory. The trajectories were started in the vicinity of the hyperbolic point $(\pi, 0)$ and iterated for a large number of time steps, N . It was verified for several cases that the results “equilibrize,” namely, they do not depend on N for large N . The correlation function is calculated from the formula

$$C_{fg}(n) = \lim_{N \rightarrow \infty} \frac{1}{N} \sum_{i=1}^N f(i)g(i+n), \quad (76)$$

where $f(j)$ and $g(j)$ are the values of f and g at the j th time step. We first calculate numerically the slow relaxation rates γ_k (70) related to diffusion and then turn to calculate and $\tilde{\gamma}$ (71) related to relaxation in the θ direction.

A. The Diffusive Modes

The relaxation rates expected from the approximate calculations of Sec. III for the diffusive modes are given by Eq. (68) or

$$\gamma_k = \frac{k^2}{s^2} D(K), \quad (77)$$

where $D(K)$ is the diffusion coefficient (4) for $\sigma=0$. To test this relation, the correlation function (74) was calculated for various distributions g and f from the Fourier basis (7) and plots like the ones presented in Fig. 1 were prepared. The slope is γ_k and the values of $D(K)$ are extracted with the help of Eq. (77) for various values of k and s . In Fig. 2 these values of $D(K)$ are depicted for large values of the stochasticity parameter K . Excellent agreement with the theory is found: (a) The value of D is found to be independent of k and s ; (b) It agrees with the theoretical prediction (4). We find indeed that for long time the behavior of distributions is indeed the same as that for a diffusive process. In the past it was found only that the second moment of the momentum grows linearly as expected for diffusion. The effect of sticking to the accelerator modes was not observed for the values of K used for Fig. 2 since the size of the accelerated region is small and therefore special effort is required to observe these effects in numerical calculations [15]. These are expected to be important for relatively small values of K where the accelerated regions are larger.

In Fig. 3 the correlation function is plotted for relatively small values of the stochasticity parameter K where larger deviations from the theory presented in Sec. III are expected. The diffusion coefficient as a function of K is presented in

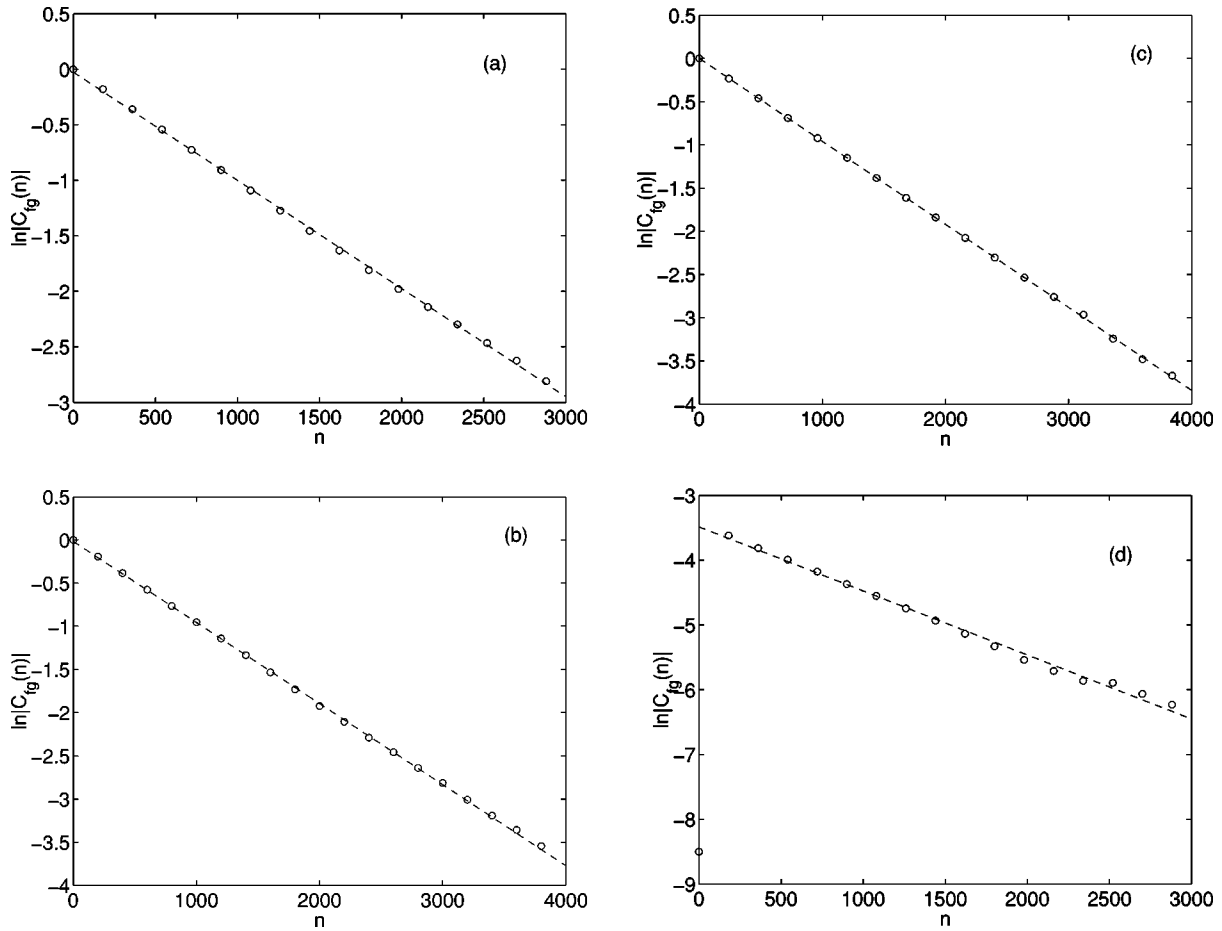


FIG. 1. The function $C_{fg}(n)$ (semilogarithmic plot) for (a) $f=g=\phi_{10}$, $K=20$, $s=370$; (b) $f=g=\phi_{20}$, $K=30$, $s=900$; (c) $f=g=\phi_{50}$, $K=40$, $s=3200$; (d) $f=\phi_{12}$, $g=\phi_{13}$, $K=27$, $s=450$. The dashed line represents the best fit to the data. The number of iterations is $N=8 \times 10^6$.

Fig. 4. Deviations of the numerical results from the analytical predictions are found for some values of K . Also for these the decay of correlations is found to be exponential and the diffusion coefficient extracted for all modes by Eq. (77) is

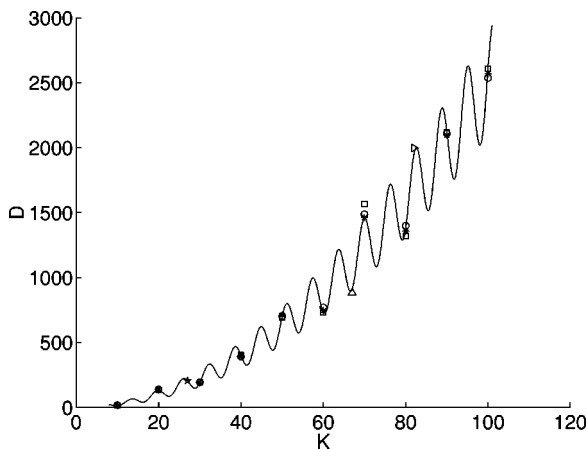


FIG. 2. The diffusion coefficient D for $K \geq 10$ as found from plots like the ones presented in Fig. 1 for the first mode [1(a)] (squares), the second mode [1(b)] (stars), the fifth mode [1(c)] (circles), correlation function for the off-diagonal first mode [1(d)] (pentagram) and other off-diagonal correlation functions (triangles), compared to the theoretical value (solid line).

the same. Therefore the behavior that is found is indeed diffusive, but the value of the diffusion coefficient for some values of K is larger than the one that is theoretically predicted. This is a result of sticking (for finite times) to accelerator modes. For most values of K the value of D found from Eq. (77) agrees with the one found from direct evaluations of trajectories in the chaotic component. The theoretical errors (marked by the dashed line in Fig. 4) were estimated from the next term of the formula of Rechester and White for the diffusion coefficient [14]. The actual errors are larger due to the nonperturbative nature of the accelerator modes and the surrounding regions (such modes cannot be found in an expansion in $1/\sqrt{K}$). Since in all calculations only trajectories belonging to the chaotic component were propagated, real acceleration is avoided. The trajectories used in the calculation of the correlation function by Eq. (76) effectively generate a projection on the chaotic component of phase space.

B. Angular Relaxation

In order to observe the angular relaxation mode it is required that no relaxation in the J direction be present, because such a relaxation, if present, would be expected to dominate the long time limit. Since the results are indepen-

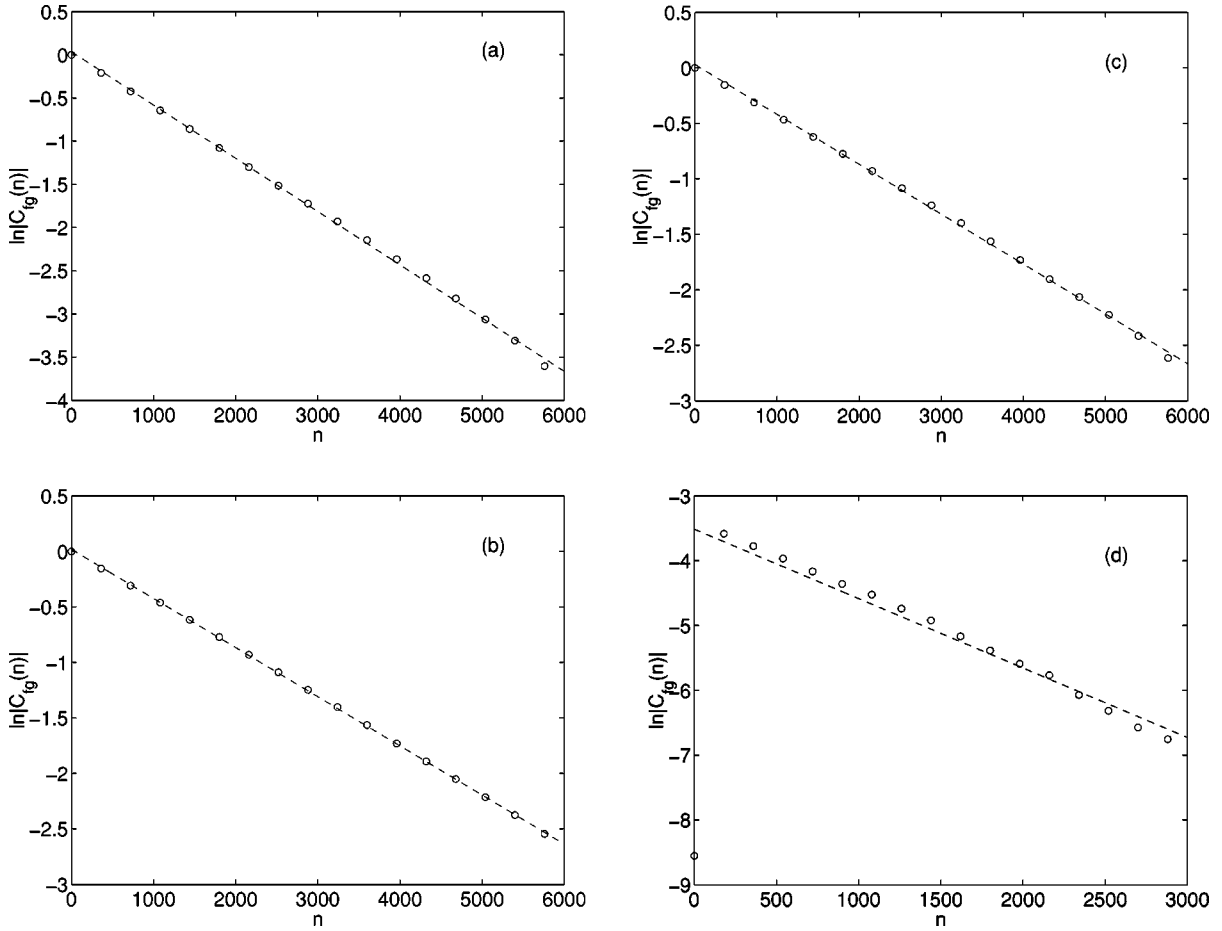


FIG. 3. The function $C_{fg}(n)$ for (a) $f=g=\phi_{10}$, $K=7$, $s=250$; (b) $f=g=\phi_{20}$, $K=8$, $s=510$; (c) $f=g=\phi_{50}$, $K=3$, $s=340$; (d) $f=\phi_{11}$, $g=\phi_{12}$, $K=17$, $s=225$. The dashed line represents the best fit to the data. The number of iterations is $N=8 \times 10^6$.

dent of s , we use $s=1$. For this purpose we take $g=\phi_{km}$ [see Eq. (7)] so that $q=k/s$ is an integer, and $f=\phi_{0m}$. From Eqs. (69) and (71) one concludes that the slowest of the angular relaxation rates is

$$\tilde{\gamma} = -\frac{1}{2} \ln[\max_{m^*} (|J_{2m^*}(m^*K)|)]. \quad (78)$$

The absolute value of the correlation function $C_{fg}(n)$ is presented in Figs. 5 and 6 for $g=\phi_{02}$ and $f=\phi_{01}$ and for $g=f=\phi_{01}$, respectively, for several values of K . The numerical calculations are complicated since the relaxation is fast, with a characteristic time of the order of one time step. Moreover, there are oscillations of the correlation function, while Eq. (78) is just the envelope. In Figs. 5 and 6 the best fit to the envelope is marked by a dashed line. The slope of the dashed line is the numerical estimate for the relaxation rate. In Fig. 7 the numerical estimate is compared with the theoretical prediction. The error in the theoretical prediction is estimated as the value of the next order contribution to a_n . This results from a term where the ‘1’s in sequences corresponding to Eqs. (63) and (65) are replaced by an ‘x’ that represents a Bessel function of order $1/\sqrt{K}$, leading to an error of the order $\ln(1 \pm 1/\sqrt{K})$ in the relaxation rate. It is difficult to estimate the error resulting from the numerical procedure of calculating the relaxation rates. The reason is that near the origin of the correlation function a large number of modes contribute. On the other hand, in the tail of the correlation function, where only one relaxation rate is dominant, the signal is too small. Nevertheless, the comparison between our numerical and theoretical results shows a good qualitative agreement.

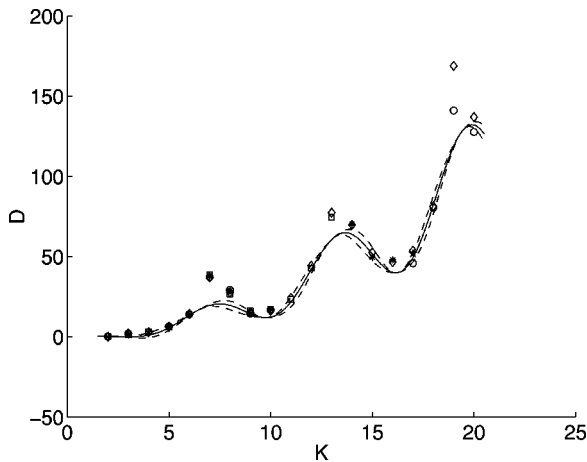


FIG. 4. The diffusion coefficient D for $K \leq 20$ as found from plots like the ones presented in Fig. 3 for the first mode [1(a)] (squares), the second mode [1(b)] (stars), the fifth mode [1(c)] (circles) and off diagonal first mode [1(d)] (pentagram), compared to the theoretical value (solid line). The dashed line represents the approximate error. The values of D obtained by direct simulation of propagation of trajectories are marked by diamonds.

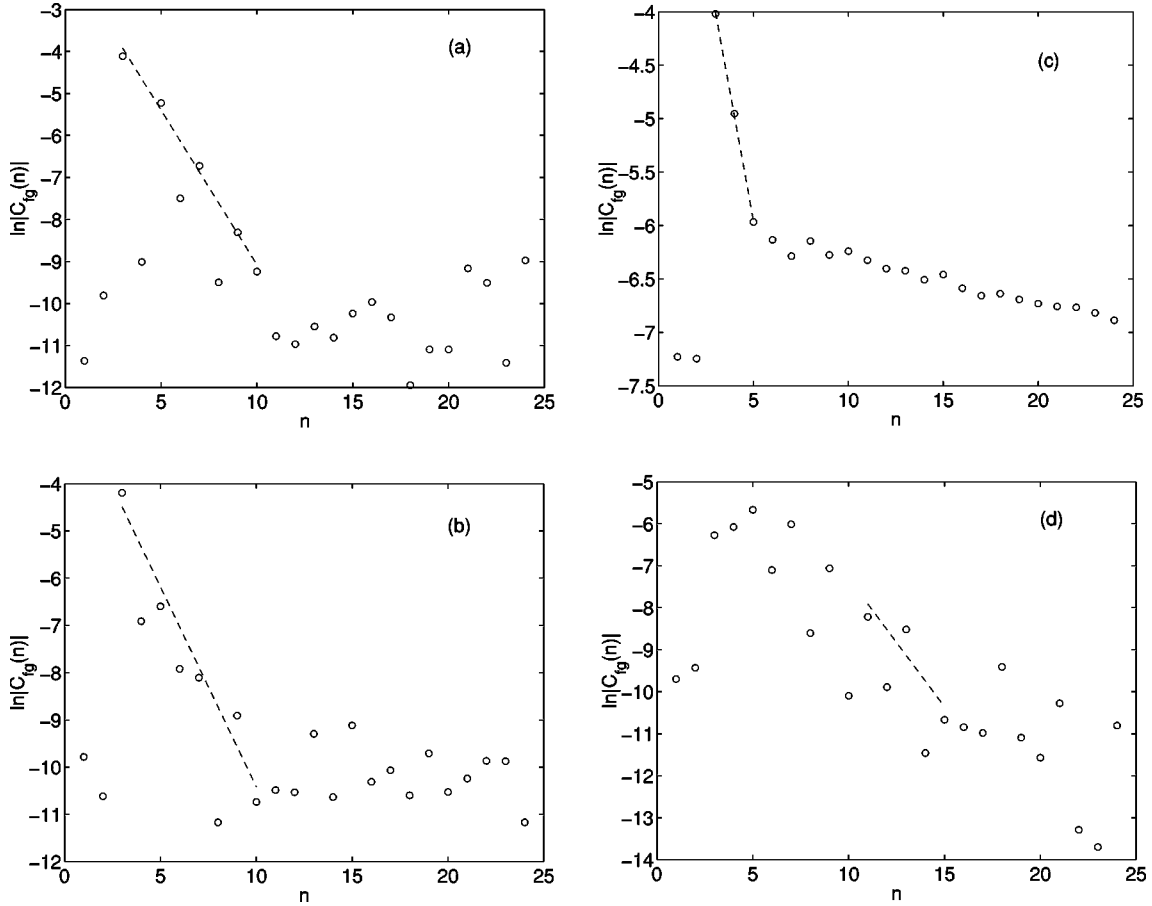


FIG. 5. The absolute value of the function $C_{fg}(n)$ for $f = \phi_{01}$, $g = \phi_{02}$ and (a) $K=16.3$, (b) $K=19.5$, (c) $K=12$, (d) $K=16$. The dashed line represents the best fit to the data. The values $s=1$ and $N=10^8$ were used.

V. SUMMARY AND DISCUSSION

Relaxation to equilibrium was studied for the kicked rotor that is a standard system for the exploration of classical chaos in driven systems and its quantum mechanical suppression. Relaxation and diffusion are important concepts in statistical mechanics. Here they were studied for a mixed chaotic system. Very little is known rigorously about such systems, although most models describing real physical systems are mixed, namely, in some regions of phase space the motion is regular while in some regions it is chaotic.

In this work the kicked rotor was studied in a phase space that is the torus defined by the inequality (6). The relaxation of distributions in phase space takes place in stages. First, the inhomogeneity in θ decays with rapid relaxation rates, the slowest of them is $\tilde{\gamma}$. Then relaxation of the inhomogeneities in the J direction takes place with the relaxation rates related to the diffusion coefficient via Eq. (77). Diffusion was previously believed to be a good approximation for the kicked rotor, but here, to the best of our knowledge, the various time scales were analyzed carefully for the first time. In particular we have found the time scale $1/\tilde{\gamma}$, below which the diffusion approximation does not hold since relaxation of correlations in the angle direction still takes place.

There is a clear relation between the relaxation of inhomogeneities in θ and the diffusion constant since

$$\langle (J_{n+1} - J_0)^2 \rangle = \sum_{i,j=0}^n K^2 \langle \sin \theta_i \sin \theta_j \rangle, \quad (79)$$

where J_i and θ_i are the momentum and angle before the i th kick. For a chaotic trajectory

$$\langle \sin \theta_i \sin \theta_j \rangle = \langle \sin \theta_0 \sin \theta_{|i-j|} \rangle = C_{ff}(|i-j|), \quad (80)$$

where $C_{ff}(|i-j|)$ is the correlation function (74) with $f = \phi_{01}$. If the sum $\sum_{i=0}^{\infty} C_{ff}(i)$ converges, as is the case where C_{ff} falls off exponentially, diffusion is found and the value of the diffusion coefficient is

$$D = \frac{K^2}{2} \sum_{i=-\infty}^{\infty} C_{ff}(i). \quad (81)$$

In Appendix C we show that Eq. (50), which was obtained by Rechester and White in [14], is just

$$D = \frac{K^2}{2} \sum_{i=-2}^2 C_{ff}(i). \quad (82)$$

A derivation that is very similar is presented in [28]. If the sum diverges one obtains anomalous diffusion.

Finite noise leads to the effective truncation of the evolution operator (21). In the basis (7) it means that it results in limited resolution. Moreover, for $\sigma > 0$ the operator \tilde{U} is nonunitary. The approximate eigenvalues of \hat{U} given by Eq. (21), which were found in this work, are 1 and z_k of Eq. (49) [if inequality (40) is satisfied] and \tilde{z} of Eq. (60). In our approximation method we could not obtain many eigenvalues

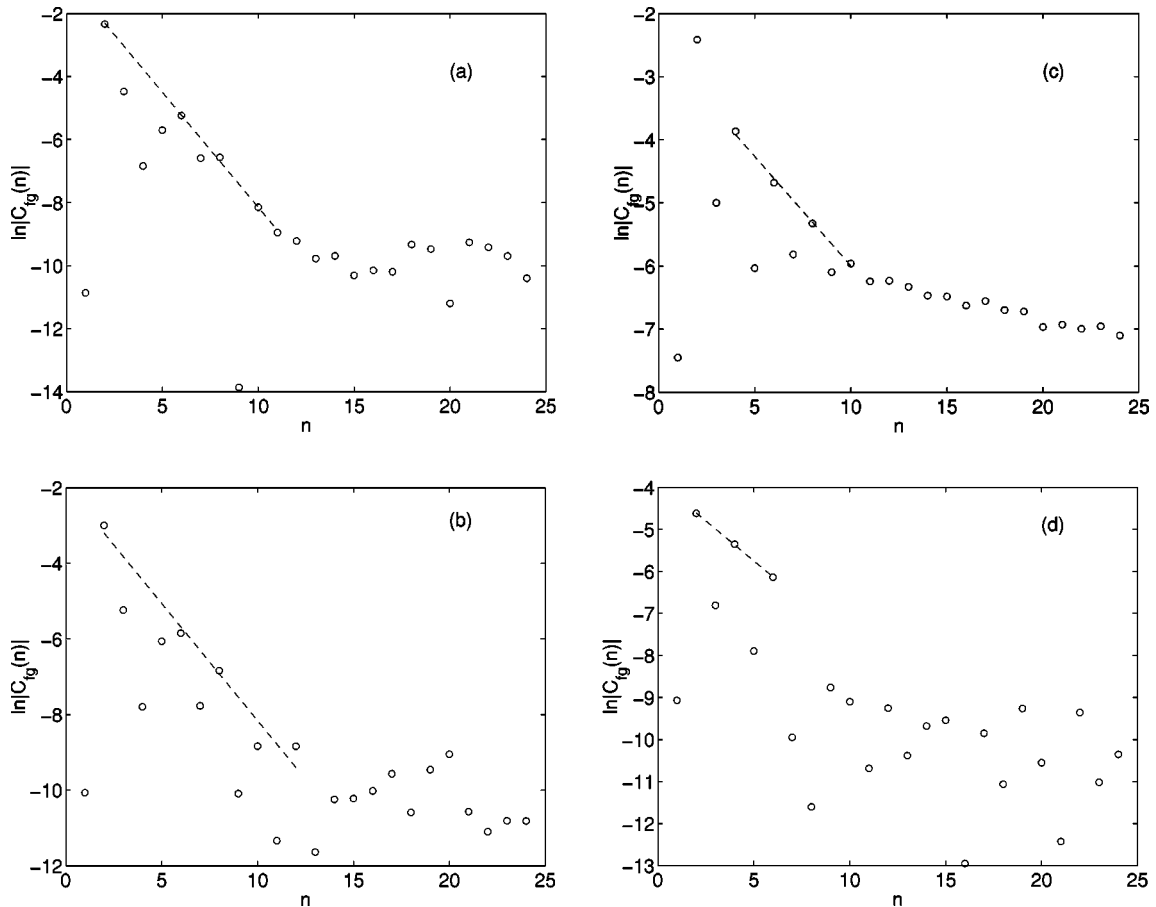


FIG. 6. The absolute value of the function $C_{fg}(n)$ for $f=g=\phi_{01}$ and (a) $K=10.7$, (b) $K=14.3$, (c) $K=12.55$, (d) $K=14.7$. The dashed line represents the best fit to the data. The values $s=1$ and $N=10^8$ were used.

related to angular relaxation modes. Because of the effective truncation ψ_γ , an eigenfunction of \hat{U} can be expanded in terms of the basis states (7). The relaxation rates of these states are $-\ln(z_k)$ and $-\ln(|\tilde{z}|)$, where z_k and \tilde{z} are given by Eqs. (49) and (66). In the limit $\sigma \rightarrow 0$, the evolution operator is unitary; ψ_γ approaches some generalized function while z_k

and \tilde{z} approach the values of the poles of the matrix elements of the resolvent \hat{R} of Eq. (25) obtained from the extrapolation from $|z| > 1$ (corresponding to the $0 < \epsilon \rightarrow 0$, which is used in the standard definition of the Green's function).

These are the Ruelle resonances that are related to the relaxation rates via Eqs. (70) and (71). This is very similar to the situation for hyperbolic systems such as the baker map. For hyperbolic systems the Ruelle resonances (related to the relaxation rates) approach fixed values inside the unit circle in the complex z plane in the limit of an infinite matrix for the evolution operator or of infinitely fine phase space resolution. This was found to be correct here also when one takes the limit $\sigma \rightarrow 0$ in Eqs. (49) and (66) resulting in Eqs. (68) and (69). Numerical tests in the absence of noise confirm that the analytical results provide a good approximation for the relaxation to equilibrium and diffusion in the chaotic component. Results of a similar nature were found in the standard map with $s=1$ for some values of K [19], for the ‘‘perturbed cat’’ map [19], and also for the kicked top [20]. In all these works it was found, within the approximations used, that the leading resonances are either real or form the quartet $(\pm A, \pm iA)$, where A is a real number satisfying $0 < A < 1$. The generality of this form should be subject to further research. For the kicked top it was attributed [20] to the dominance of an orbit of period 4.

In mixed systems, such as the kicked rotor, even in the chaotic components there is sticking to regular islands and

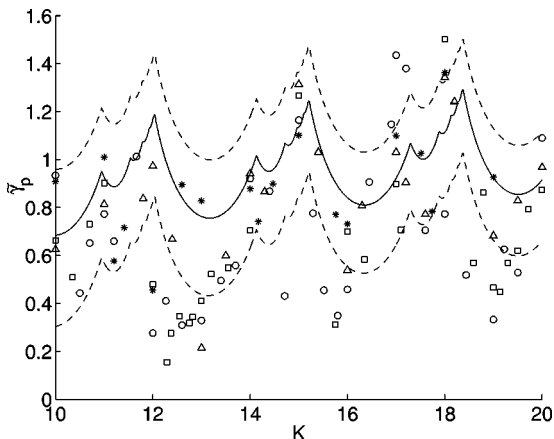


FIG. 7. The fast relaxation rate $\tilde{\gamma}$ as found from plots like Figs. 5 and 6 for $f=\phi_{01}$, $g=\phi_{02}$ (triangles), $f=\phi_{02}$, $g=\phi_{04}$ (circles), $f=g=\phi_{02}$ (stars) and $f=g=\phi_{01}$ (squares), compared to the theoretical value (78) (solid line). The dashed lines denote the theoretical estimated error. Here we used $s=1$ and $N=10^8$.

acceleration modes. Noise eliminates this sticking. The analytic formulas (68) and (69) are obtained from an expansion in powers of $1/\sqrt{K}$ for a finite variance of noise σ^2 and the limit $\sigma^2 \rightarrow 0$ is taken in the end of the calculation. A nonvanishing value of σ^2 assures the convergence of the series (57). Appearance of the islands and the sticking are nonperturbative effects and therefore are not reproduced in our theory. For this reason, in the absence of noise the results are only approximate. The effect of the sticking is extremely small for most values of the stochasticity parameter K , as verified by the numerical calculations without noise.

The physical reason for the decay of the correlations is that in a chaotic system, because of the stretching and folding mechanisms, there is persistent flow in the direction of functions with finer details, namely, larger $|k|$ and $|m|$ in our case. Consequently, the projection on a given function, for example one of the basis functions (7) in our case, decays [20,29]. The crucial point is that this function should be sufficiently smooth. This argument should also hold for the chaotic component of mixed systems. In the present paper the actual relaxation rates were calculated. Here noise was used in order to make the analytical calculations possible. In real experiments some level of noise is present, therefore the results in the presence of noise are of experimental relevance. It was shown with the help of the Cauchy-Hadamard theorem [27] [see the discussion following Eq. (32)] that for $s \gg K \gg 1$ exponential relaxation to the invariant density takes place with the rate $\gamma_1 = D(K)/s^2$, where $D(K)$ is given by Eq. (4). It was deduced from the radius of convergence for the series of the matrix element of \hat{R}' [see Eq. (29)]. This rate is independent of σ . It is found for all functions that can be expanded in the basis (7), with an absolutely convergent expansion. It excludes, for example, functions of the form (22). We believe this statement can be made rigorous by experts.

For the baker map it was found that the resolvent of the evolution operator of the quantum Wigner function, when coarse grained, has the same poles as the classical Frobenius-Perron operator [21]. We believe it should also hold here. The fact that the Ruelle resonances of the modes of slow relaxation are z_k , which are identical to the ones of the diffusion operator, gives additional support to approximations made for the calculation of the ensemble averaged localization length in [24].

Finally, the Ruelle resonances, which were introduced and established rigorously for hyperbolic systems, can be used to describe relaxation and transport in the chaotic component of mixed systems. Here it was demonstrated for the kicked rotor.

ACKNOWLEDGMENTS

We have benefited from discussions with E. Berg, R. Dorfman, I. Guarneri, F. Haake, E. Ott, R. Prange, S. Rahav, J. Weber, and M. Zirenbauer. We thank in particular D. Alonso for extremely illuminating remarks and helpful suggestions. This research was supported in part by the US-NSF Grant No. NSF DMR 962 4559, the U.S.-Israel Binational Science Foundation (BSF), by the Minerva Center for Non-linear Physics of Complex Systems, by the Israel Science Foundation, by the Niedersachsen Ministry of Science (Germany)

and by the Fund for the Promotion of Research at the Technion. One of us (S.F.) would like to thank R.E. Prange for the hospitality at the University of Maryland, where this work was completed.

APPENDIX A: MATRIX ELEMENTS OF THE EVOLUTION OPERATOR IN THE PRESENCE OF NOISE

In this appendix the matrix elements in the representation (7) are calculated. For this purpose Eq. (20) is transformed to the Fourier representation by

$$\begin{aligned} (k_2 m_2 | \hat{U} | k_1 m_1) &= \int_0^{2\pi} d\theta \int_0^{2\pi s} dJ \int_0^{2\pi} d\theta' \int_0^{2\pi s} dJ' (k_2 m_2 | J\theta) \\ &\quad \times (J\theta | \hat{U}_{noise} | J'\theta') (J'\theta' | \hat{U}_K | k_1 m_1). \end{aligned} \quad (A1)$$

Substitution of Eqs. (18) and (19) yields

$$\begin{aligned} (k_2 m_2 | \hat{U} | k_1 m_1) &= \int_0^{2\pi} d\theta \int_0^{2\pi s} dJ \int_0^{2\pi} d\theta' \frac{1}{\sqrt{2\pi}} \frac{1}{\sqrt{2\pi s}} \\ &\quad \times \exp(-im_2\theta) \exp\left(i\frac{-k_2 J}{s}\right) \\ &\quad \times \sum_m \frac{1}{2\pi} \exp(im(\theta' - \theta)) \\ &\quad \times \exp\left(-imJ - \frac{\sigma^2}{2} m^2\right) \frac{1}{\sqrt{2\pi}} \frac{1}{\sqrt{2\pi s}} \\ &\quad \times \exp(im_1\theta') \exp\left(i\frac{k_1}{s}(J + K \sin \theta')\right). \end{aligned} \quad (A2)$$

Terms containing θ are $\exp(im(-\theta))\exp(-im_2\theta)$. Integration over θ yields $\delta_{m,-m_2}$ leading to

$$\begin{aligned} (k_2 m_2 | \hat{U} | k_1 m_1) &= \int_0^{2\pi s} dJ \int_0^{2\pi} d\theta' \frac{1}{\sqrt{2\pi s}} \exp\left(i\frac{-k_2 J}{s}\right) \\ &\quad \times \frac{1}{2\pi} \exp(-im_2\theta') \\ &\quad \times \exp\left(im_2 J - \frac{\sigma^2}{2} m_2^2\right) \frac{1}{\sqrt{2\pi s}} \\ &\quad \times \exp(im_1\theta') \exp\left(i\frac{k_1}{s}(J + K \sin \theta')\right). \end{aligned} \quad (A3)$$

Integration over J results in $\delta_{k_2 - k_1, m_2 s}$, yielding

$$\begin{aligned}
(k_2 m_2 | \hat{U} | k_1 m_1) &= \frac{1}{2\pi} \int_0^{2\pi} d\theta' \exp(-i(m_2 - m_1)\theta') \\
&\times \exp\left(-\frac{\sigma^2}{2} m_2^2\right) \\
&\times \exp\left(i \frac{k_1}{s} K \sin \theta'\right) \delta_{k_2 - k_1, m_2 s}. \quad (\text{A4})
\end{aligned}$$

Finally, with the help of the integral representation for Bessel functions:

$$J_m(z) = \frac{1}{2\pi} \int_0^{2\pi} d\theta \exp(-im\theta) \exp(iz \sin \theta),$$

one obtains Eq. (21).

APPENDIX B: END TERMS IN STRINGS OF THE FAST MODES

In this appendix, possible examples for contributions to the end terms in the expression (65) are presented. The left end term is a sum of terms of the form

$$\begin{aligned}
C^{(l)}(m, m^*) &= J_{2m+m^*}(-mK) J_{-m-2m^*}(m^*K) J_0(0) \\
&\times \exp\left[-\frac{\sigma^2}{2}(m^2 + (m+m^*)^2 + m^{*2})\right] \\
&+ \sum_{m_1} J_{m-m_1}(-mK) J_{2m_1+m+m^*}((-m-m_1)K) \\
&\times J_{-m-2m^*-m_1}(m^*K) J_0(0) \\
&\times \exp\left[-\frac{\sigma^2}{2}(m^2 + m_1^2 + (m+m^*+m_1)^2 + m^{*2})\right] \dots, \quad (\text{B1})
\end{aligned}$$

where in the first term $m_1 = (m + m^*)$ and $m_2 = m_3 = m^*$, while in the second term $m_2 = -(m + m^* + m_1)$ and $m_3 = m_4 = m^*$. For $q \neq 0$ the right end term is a sum of terms of the form

$$\begin{aligned}
C^{(r)}(m^*, m', q) &= \sum_{m_{n-1}} J_{2m^*+m_{n-1}+q}(-m^*K) \\
&\times J_{-m^*-2m_{n-1}-q}((m_{n-1}+q)K) J_{m_{n-1}-m'}(qK) \\
&\times \exp\left[-\frac{\sigma^2}{2}(m^{*2} + (m^*+m_{n-1}+q)^2 + m_{n-1}^2)\right] \dots, \quad (\text{B2})
\end{aligned}$$

where $m_{n-2} = -(m^* + m_{n-1} + q)$ and $m_{n-3} = m^*$. For $q = 0$ one has to take $m_{n-1} = m'$ and the end term consists of a sum over m_{n-2} .

APPENDIX C: RELATION BETWEEN THE DIFFUSION COEFFICIENT AND CORRELATION FUNCTION

In this appendix the relation between Eqs. (82) and (50) will be derived (for a somewhat similar derivation see [28]). For this purpose we note that

$$\begin{aligned}
C_{ff}(n) &= \int_0^{2\pi} \frac{d\theta}{2\pi} \int_0^{2\pi s} \frac{dJ}{2\pi s} \sin \theta \hat{U}^n \sin \theta \\
&= -\frac{1}{4} [(0, -1 | - (0, 1 |] \hat{U}^n [|0, 1 \rangle - |0, -1 \rangle], \quad (\text{C1})
\end{aligned}$$

where the representation $|k, m\rangle$ [see Eq. (7)] is used. The matrix elements of \hat{U} are given by Eq. (21) and the matrix elements of \hat{U}^2 required for the present calculation are

$$(0, m_2 | \hat{U}^2 | 0, m_1) = J_{2m_2}(-m_2 K) e^{-\sigma^2 m_2^2} \delta_{m_1, -m_2}, \quad (\text{C2})$$

as can be easily obtained from the multiplication of two matrices of the form (21). From Eq. (C1) it is clear that $C_{ff}(0) = \frac{1}{2}$. Inspecting Eq. (21) with $k_1 = k_2 = 0$, one notes that it is required that also $m_1 = m_2 = 0$, therefore $C_{ff}(1) = 0$. Substitution of Eq. (C2) in Eq. (C1) yields

$$C_{ff}(2) = -\frac{1}{2} J_2(K) e^{-\sigma^2}. \quad (\text{C3})$$

Using the fact that $C_{ff}(-n) = C_{ff}(n)$, substitution of the values of $C_{ff}(0)$ and $C_{ff}(2)$ into Eq. (82) yields the expression (50) that was obtained by Rechester and White [14]. Because of the discussion following the expression (59) the correlation functions $C_{ff}(n)$ with $n > 2$ lead to terms that are of higher orders in $1/\sqrt{K}$ than Eq. (50).

-
- [1] E. Ott, *Chaos in Dynamical Systems* (Cambridge University Press, Cambridge, 1997).
[2] V. I. Arnold and A. Avez, *Ergodic Problems of Classical Mechanics* (Addison-Wesley, New York, 1989).
[3] P. Gaspard, *Chaos, Scattering and Statistical Mechanics* (Cambridge University Press, Cambridge, 1998).
[4] J. R. Dorfman, *An Introduction to Chaos in Non-Equilibrium Statistical Mechanics* (Cambridge University Press, Cambridge, 1999).
[5] D. Ruelle, *Statistical Mechanics, Thermodynamic Formalism* (Addison-Wesley, Reading, MA, 1978); Phys. Rev. Lett. **56**,

- 405 (1986).
[6] P. Cvitanović and B. Eckhardt, J. Phys. A **24**, L237 (1991).
[7] P. Gaspard, Phys. Rev. E **53**, 4379 (1996).
[8] A. J. Lichtenberg and M. A. Lieberman, *Regular and Stochastic Motion* (Springer, New York, 1983).
[9] B. V. Chirikov, Phys. Rep. **52**, 263 (1979).
[10] R. Balescu, *Statistical Dynamics, Matter out of Equilibrium* (Imperial College Press, Singapore, 1983).
[11] G. Casati, B. V. Chirikov, F. M. Izrailev, and J. Ford, Lect. Notes Phys. **93**, 334 (1979).
[12] S. Fishman, D. R. Grempel, and R. E. Prange, Phys. Rev. Lett.

- 49, 509 (1982); D. R. Grempel, R. E. Prange, and S. Fishman, Phys. Rev. A **29**, 1639 (1984).
- [13] S. Fishman, in *Quantum Dynamics of Simple Systems*, Proc. of the 44th Scottish Universities Summer School in Physics, Stirling, Aug. 1994, edited by G.-L. Oppo, S. M. Barnett, E. Riis, and M. Wilkinson (SUSSP Publications and Institute of Physics, Bristol, 1996).
- [14] A. B. Rechester and R. B. White, Phys. Rev. Lett. **44**, 1586 (1980); A. B. Rechester, M. N. Rosenbluth, and R. B. White, Phys. Rev. A **23**, 2664 (1981); E. Doron and S. Fishman, *ibid.* **37**, 2144 (1988).
- [15] S. Benkadda, S. Kassibrakis, R. B. White, and G. M. Zaslavsky, Phys. Rev. E **55**, 4909 (1997); G. M. Zaslavsky, J. Plasma Phys. **59**, 671 (1998); G. M. Zaslavsky and B. A. Niyazov, Phys. Rep. **283**, 73 (1979); B. Sundaram and G. M. Zaslavsky, Phys. Rev. E **59**, 7231 (1999); G. M. Zaslavsky, M. Edelman, and B. A. Niyazov, Chaos **7**, 1 (1997).
- [16] A short version of this work is presented in M. Khodas and S. Fishman, Phys. Rev. Lett. **84**, 2837 (2000); Erratum, *ibid.* **84**, 5918 (2000).
- [17] H. H. Hasegawa and W. C. Saphir, Phys. Rev. A **46**, 7401 (1992).
- [18] I. Antoniou, B. Qiao, and Z. Suchanecki, Chaos, Solitons Fractals **8**, 77 (1997); J. Wilkie, A. Pattanayak, and P. Brumer, Chaos, Solitons, and Fractals **11**, 1473 (2000).
- [19] G. Blum and O. Agam, Phys. Rev. E **62**, 1977 (2000).
- [20] J. Weber, F. Haake, and P. Šeba (unpublished); (private communication).
- [21] S. Fishman, in *Supersymmetry and Trace Formulae, Chaos and Disorder*, edited by I. V. Lerner, J. P. Keating, and D. E. Khmelnitskii (Kluwer Academic / Plenum, New York, 1999), p. 193.
- [22] M. R. Zirnbauer, in *Supersymmetry and Trace Formulae, Chaos and Disorder*, edited by I. V. Lerner, J. P. Keating, and D. E. Khmelnitskii (Kluwer Academic / Plenum, New York, 1999), p. 153.
- [23] A. V. Andreev and B. L. Altshuler, Phys. Rev. Lett. **75**, 902 (1995); O. Agam, B. L. Altshuler, and A. V. Andreev, *ibid.* **75**, 4389 (1995); A. V. Andreev, O. Agam, B. D. Simons, and B. L. Altshuler, *ibid.* **76**, 3947 (1996); Nucl. Phys. B **482**, 536 (1996); Phys. Rev. Lett. **79**, 1778 (1997); O. Agam, A. V. Andreev, and B. D. Simons, Chaos, Solitons Fractals **8**, 1099 (1997); J. Math. Phys. **38**, 1982 (1997).
- [24] A. Altland and M. R. Zirnbauer, Phys. Rev. Lett. **77**, 4536 (1996); **80**, 641 (1998).
- [25] G. Casati, F. M. Israilev, and V. V. Sokolov, Phys. Rev. Lett. **80**, 640 (1998).
- [26] M. V. Berry, in *New Trends in Nuclear Collective Dynamics*, edited by Y. Abe, H. Horiuchi, and K. Matsuyanagi, Springer Proc. Phys. **58**, 183 (1992).
- [27] K. Knopp, *Infinite Sequences and Series* (Dover, New York, 1956).
- [28] J. R. Cary, J. D. Meiss, and A. Bhattacharee, Phys. Rev. A **23**, 2744 (1981).
- [29] F. Haake (unpublished).